ADVANCED MATERIALS
www.advmat.de

The Optical Janus Effect: Asymmetric Structural Color Reflection Materials

*Grant T. England, Calvin Russell, Elijah Shirman, Theresa Kay, Nicolas Vogel, and Joanna Aizenberg**

Structurally colored materials are often used for their resistance to photobleaching and their complex viewing-direction-dependent optical properties. Frequently, absorption has been added to these types of materials in order to improve the color saturation by mitigating the effects of nonspecific scattering that is present in most samples due to imperfect manufacturing procedures. The combination of absorbing elements and structural coloration often yields emergent optical properties. Here, a new hybrid architecture is introduced that leads to an interesting, highly directional optical effect. By localizing absorption in a thin layer within a transparent, structurally colored multilayer material, an optical Janus effect is created, wherein the observed reflected color is different on one side of the sample than on the other. A systematic characterization of the optical properties of these structures as a function of their geometry and composition is performed. The experimental studies are coupled with a theoretical analysis that enables a precise, rational design of various optical Janus structures with highly controlled color, pattern, and fabrication approaches. These asymmetrically colored materials will open applications in art, architecture, semitransparent solar cells, and security features in anticounterfeiting materials.

For thousands of years, humans have been fascinated with the panoply of colors found in nature, and have sought to create materials that exhibit these colors in a variety of ways. Throughout this time, there has been continual improvement in the ability to fabricate and understand the underlying physics of these structures, from the 4th century Roman Lycurgus cup,[1] showing different color in reflection and transmission, to the inspiring coloration of ancient church windows,[2] and modern effect pigments[3] that use sparkle, luster, and color travel to create vivid coloration. Aesthetics and function are often intimately linked in modern materials.[4] Examples can be found in materials that change color to indicate structural fatigue in bridges, buildings, or airplane wings.[5] or modify transparency to allow energy savings,[6] as well as in the fields of anticounterfeiting,[7,8] solar-energy harvesting, modulation of absorption and thermal emission,[9] and colorimetric sensing.[10]

Generally, the coloration of a material results from a combination of absorption, reflection, and scattering. Absorption of light in a given wavelength range leads to a macroscopic color; for example, by electronic excitations in dyes or plasmonic resonances in noble metal nanoparticles.[11,12] Alternatively, micro-to-nanoscale structured materials can enable optical interference phenomena, resulting in structural coloration. Examples of structural coloration abound in natural species,[13] and can also be found in synthetic photonic structures such as diffraction gratings,[7,14] colloidal crystals,[15] and multilayer stacks.[16]

The combination of structural coloration and absorption can improve the color saturation of materials by reducing the amount of nonspecific background scattering in the structure. In the simplest case, absorbers—whether dyes or plasmonic particles—are used to purify the spectrum of structurally colored materials, especially by distributing an absorber homogeneously throughout the material.[17] The controlled localization of the absorbing moieties within a composite architecture can provide avenues for completely new optical effects. Examples include ultrathin perfect absorbers,[18] ultrathin-film semiconductor/metal structural color materials,[9] antireflective coatings,[19] structural color saturation adjustment,[20] and asymmetric reflection materials.[21,22] Strikingly, asymmetric absorption properties can arise from the combination of an absorbing layer with a thin film. In particular, combining two structural color elements (a thin film and a plasmonic metamaterial) with an absorbing layer (a film of silver) can lead to asymmetric absorption properties at specific wavelengths.[21]

A material with such an asymmetric absorption spectrum, by conservation of energy, must have an asymmetric reflection

Dr. G. T. England, C. Russell, Dr. E. Shirman, Prof. J. Aizenberg
John A. Paulson School of Engineering and Applied Sciences
Harvard University
Cambridge, MA 02138, USA
E-mail: jaiz@seas.harvard.edu
Dr. E. Shirman, T. Kay, Prof. J. Aizenberg
Wyss Institute for Biologically Inspired Engineering
Harvard University
Cambridge, MA 02138, USA
Prof. N. Vogel
Institute of Particle Technology
Friedrich-Alexander University Erlangen-Nürnberg
Cauerstrasse 4, 91058 Erlangen, Germany
Prof. J. Aizenberg
Department of Chemistry and Chemical Biology
Harvard University
Cambridge, MA 02138, USA

DOI: 10.1002/adma.201606876

spectrum. We anticipated that by generalizing the system of a structural color material and an absorbing layer, which can impart an anomalous phase shift (one different from 0 or π) on the reflected light, one can rationally design the reflected color from one side of the material to be arbitrarily different from the reflected color from the opposite side. Here, we develop this idea to create semitransparent coatings that exhibit different reflected colors depending on the viewing direction. In analogy to Janus particles[23] that feature different chemical compositions on either side, we will refer to these materials as optical Janus materials to highlight the asymmetric nature of their reflection. We investigate the underlying physical origin of the observed effect, provide general design guidelines to create coatings with arbitrary reflection colors from each side, and use patterning techniques to create optical Janus patterns with viewing-direction-dependent optical properties.

We fabricate optical Janus thin films using gold nanoparticles ($d \approx 12$ nm) as an absorbing element in combination with a sputter-coated titania thin film ($d = 218$ nm) used as the photonic element causing thin film interference (see Figure S1 of the Supporting Information for fabrication details and for nanoparticles characterization). In **Figure 1**, we compare the viewing-direction-dependent optical properties of the thin film to a reference sample without any absorbing gold nanoparticles and a sample with gold nanoparticles deposited at the air/titania interface. As expected, the color observed from either side of the thin film without an absorbing material has an identical light pink hue (Figure 1a), whereas that observed on the sample with the absorbing layer between the substrate and the dielectric shows a strong difference in the color, appearing bright cyan when viewed from the film side and deep violet when viewed from the substrate side (Figure 1b). The drastic difference between the color observed in these two configurations is further emphasized by the measured reflectance spectra (dashed lines, Figure 1b). If the gold nanoparticles are deposited at the air/titania interface, only slight differences exist in the reflected intensity of the spectrum, but not in the location of the peak and trough wavelengths (Figure 1c).

We attribute the observed asymmetric reflection properties to the absorbing metal nanoparticles' effective complex refractive index (RI), which is very sensitive to their dielectric environment.[12] This complex RI is then manifested in anomalous phase shifts occurring upon the reflection from an absorbing layer, as predicted by the Fresnel reflection coefficient for normal incidence:[24]

$$r_{1,2} = \frac{\tilde{n}_1 - \tilde{n}_2}{\tilde{n}_1 + \tilde{n}_2} \tag{1}$$

where $\tilde{n}_1, \tilde{n}_2$ are the complex RIs of the incident and reflecting media, respectively, with the imaginary part of the RI representing the loss or gain of the material. For non-normal incidence, these coefficients are different for the transverse electric and transverse magnetic polarizations; for simplicity, we assume normal incidence for all calculations. It can easily be seen that when there is no absorption, the Fresnel coefficient will be purely real, and therefore will cause either a 0 or π phase change in the reflected light (**Figure 2**a). In a conventional thin film with an RI higher than that of the substrate, there will be no phase shift for the internal reflections. Thus, the total phase accumulated for a given path is the same regardless of the incident direction: the resulting reflected structural color observed from either side of the material is identical. However, when one or both of the media have complex RIs, the Fresnel reflection coefficient becomes complex, and therefore imparts an anomalous phase shift (deviating from 0 or π) on the reflected light (Figure 2b). Since the RIs of the materials on either side of the absorbing layer are different, the accumulated phase is no longer the same for light incident from either side of the structure and we can expect to see the optical Janus effect.

From these simple arguments, we calculate the strength of the optical Janus effect based on the anomalous phase changes

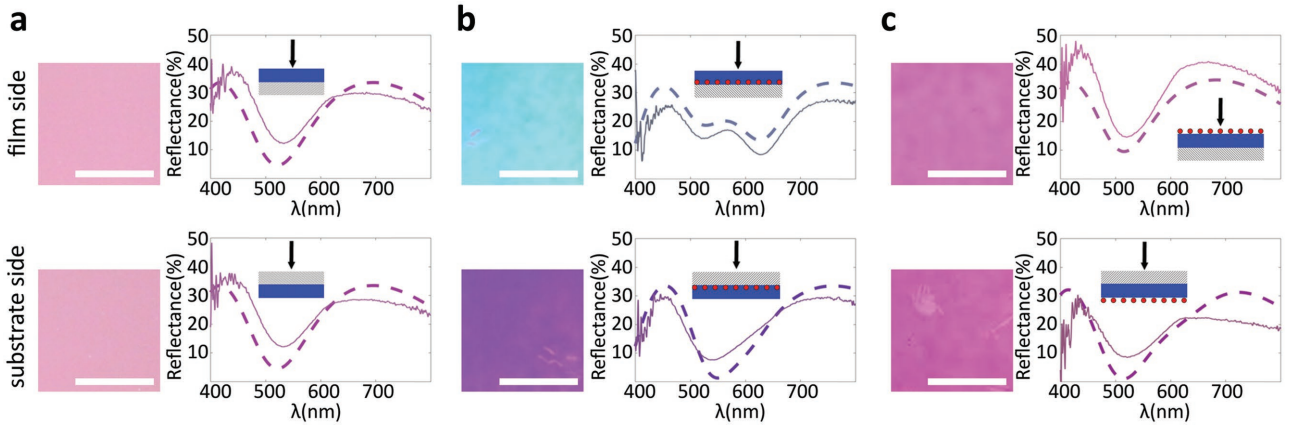

Figure 1. The optical Janus effect observed in a thin film architecture. a) (Film side) photographic image of a titania (≈218 nm) thin film on a glass substrate (left), with simulated (dashed) and measured (solid) reflectance spectra (right), measured from the film side of the sample. The color of each curve is calculated from the CIE (International Commission on Illumination) 1931 color matching functions. The inset in the spectra shows the sample configuration and observation direction. (Substrate side) same as above, but for the sample measured from the substrate side of the sample. b) Same as (a) but for a thin film containing gold nanoparticles located at the substrate/thin film interface (shown as red dots in the schematics). c) Same as (b) but with the nanoparticles located at the air/thin film interface. All scale bars are 1 cm.

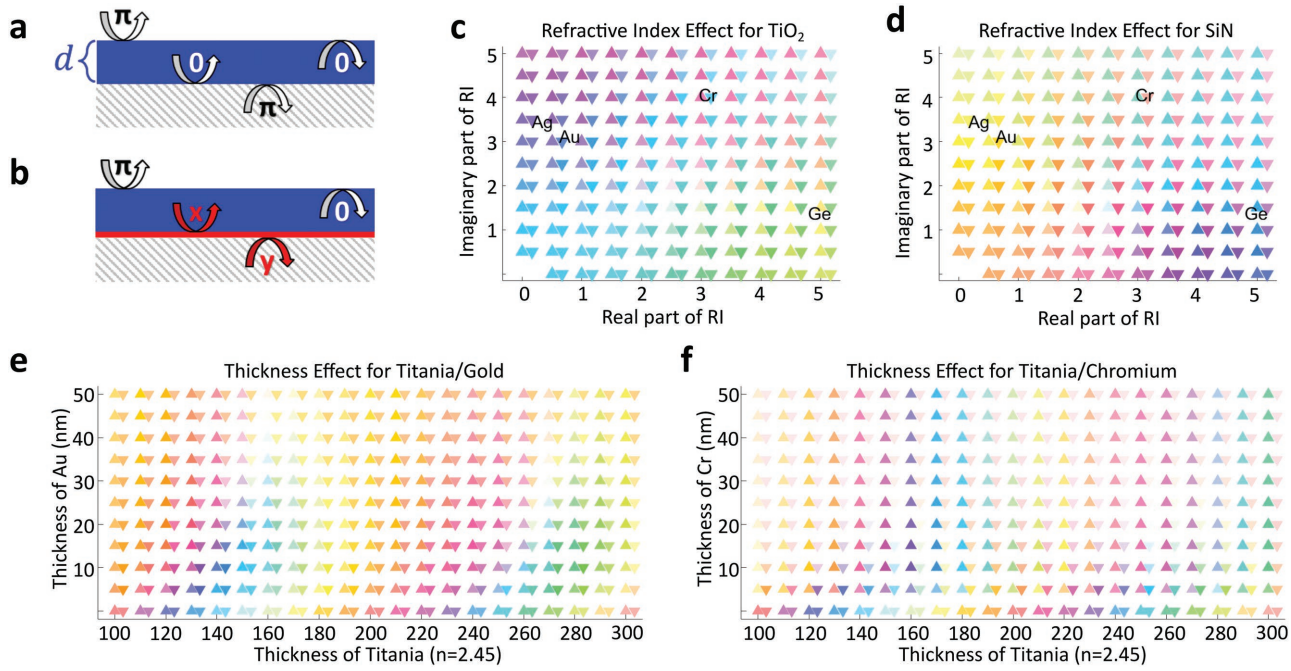

Figure 2. Janus effect simulations and theory. a,b) Schematic showing the anomalous phase shift upon reflection from a thin absorbing layer (red) in a thin film material (blue) on a transparent substrate (hatched). The refractive index (RI) of the thin film material is assumed to be higher than that of the substrate. a) Illustration showing the phase changes of 0 and 2π upon external and internal reflections of a dielectric layer. b) Same as (a) but for a dielectric film deposited on an absorbing layer showing anomalous reflection phase changes from the absorbing interfaces. c) Transfer matrix-calculated film-side (upward triangles) and substrate-side (downward triangles) reflectance color for a 250 nm film of titania ($n = 2.45$) with a 7 nm absorbing layer at the bottom on a glass substrate for various real and imaginary parts of the RI of the absorbing layer. The color of each triangle is calculated from its spectrum using the CIE 1931 color matching functions. The average real and imaginary RIs over the visible spectrum of different absorbing materials are inserted into the diagram. d) Same as (c) but for a 250 nm film of SiN (RI = 1.95). e) Same as (c) for a thin film of titania on gold on a glass substrate ($n = 1.54$) with varying thicknesses of the titania and gold layers. f) Same as (e) for titania on chromium on glass.

upon reflection from thin film (α) and substrate side (β). We use the transfer matrix method and vary the real and imaginary part of the RI of an absorbing layer, which we model as a thin absorbing film placed underneath the photonic thin film.[24] Figure 2c,d shows exemplified analytical solutions for thin-film structures made of 250 nm of titania (Figure 2c) or silicon nitride (Figure 2d), each of which has a thin absorbing layer (7 nm) with a varying complex RI at the substrate/thin-film interface. The triangle pointing up is colored with the simulated human-eye perceived color as observed from the film side of the sample, while the triangle pointing down is the same for the sample observed from the substrate side. The strongest structural color asymmetry, i.e., the biggest color change for different viewing directions, can be observed for high real and imaginary parts of the RI of the absorbing element (the positions of exemplary metals are superimposed on the graphs). This can be clearly seen in Figure S2 (Supporting Information), which shows the difference in the hue of the color from the two sides of the structures simulated in Figure 2c,d.

These analytical calculations explain the dependence of the observed optical Janus effect on the location of the absorbing element shown in Figure 1a–c. If the absorbing gold nanoparticle layer is positioned at the air/thin-film interface, the surrounding material is air, so the real part of the effective RI of the absorbing layer is low. Moreover, the localized surface plasmon resonance of gold nanoparticles experiences spectral shifts when they are surrounded by a lower index material—causing a blueshift and a decrease in intensity of the absorbance peak—which lowers the imaginary part of the RI of the absorbing layer.[12] Both effects weaken the optical asymmetry and cause similar reflection colors from either side of the sample (Figure 1c). In contrast, placing the gold nanoparticle layer in between the substrate and the dielectric film increases both the real and imaginary part of the effective RI of the absorbing layer, leading to a pronounced structural color asymmetry (Figure 1b).

Furthermore, we can calculate the effect of the thickness of both the absorbing and the dielectric films on the reflected color. As an example, we choose gold (Figure 2e) and chromium (Figure 2f) to contrast the strength of the effect for metals with different complex RIs and skin depths. While even a slight shift in the thickness of the gold layer will change the observed colors and reduce the asymmetry of the effect, a strong difference in color from the two sides is clearly observable for all thicknesses of chromium down to 5 nm. The three fundamental configurations shown in Figure 1, along with the simulations shown in Figure 2, demonstrate the key parameters in designing coatings with asymmetric structural coloration: the presence of an absorbing element, its position relative to the other optical elements, and its complex refractive index.

Coatings with asymmetric color reflection are not limited to thin films but can also be prepared from multilayer architectures, allowing for an increase in overall reflectivity and more control of the optical spectra. Figure S3 (Supporting

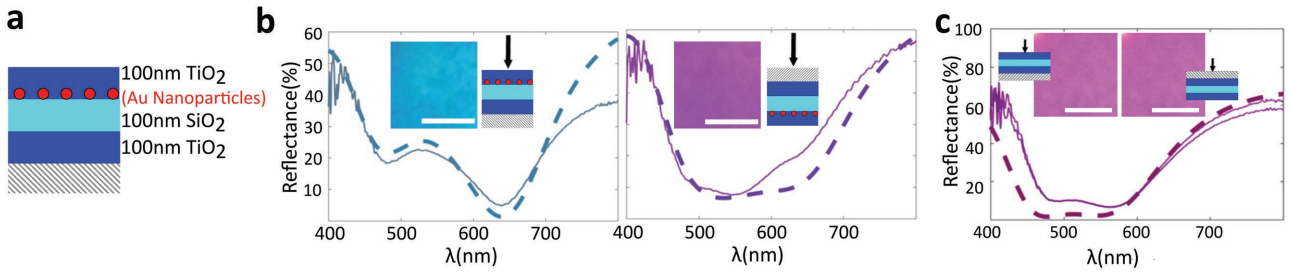

Figure 3. The optical Janus effect observed in a multilayer stack. a) Schematic showing the deposited film thicknesses of the samples in (b). b) Simulated (dashed) and measured (solid) reflectance spectra for sample in (a) with nanoparticles observed from the film side (left) and substrate side (right). Insets show the viewing direction and optical images of the sample. The color of each curve is calculated from the CIE 1931 color matching functions. All scale bars are 1 cm. c) Same as (b) for sample in (a) without the gold nanoparticles. The optical properties are identical from both viewing directions.

Information) provides transfer matrix-calculated reflectance colors for exemplary multilayer stacks. Incorporation of a gold nanoparticle layer into the high RI part of the multilayer structure results in a strong optical Janus effect with a pronounced dissimilarity of observed color depending on the viewing direction (**Figure 3**a,b). Similar to the thin film architecture, a multilayer without an absorbing layer always shows the same color when observed from both sides (Figure 3c; Figure S3, Supporting Information). When changing the location of the nanoparticles within the multilayer, the effect can be enforced or diminished, depending on the RI of the layer embedding the absorbing nanoparticles (Figure S4 and S5, Supporting Information).

In **Figure 4**, we show micrometer-scale structures with patterned, viewing-direction-dependent optical properties by controlling the spatial positioning of the absorbing elements using photolithographic techniques. We deposit a thin gold film on a photolithographic pattern and apply a lift-off technique to remove the gold film from prepatterned structures (see Figure S6, Supporting Information). A dewetting process at 500 °C subsequently transforms the gold film into separated nanoislands[25] at predefined areas (Figure 4a,b; Figure S7, Supporting Information). After deposition of a multilayer structure (Figure 4e) as the photonic element, only the nanoparticle-coated areas exhibit the optical Janus effect, while all other areas show direction-independent color determined by the photonic stack (Figure 4c,d): the color of the predefined pattern in Figure 4c,d changes from orange to green when viewed from the film side and substrate side, respectively, while the background remains uniformly yellow. A slight modification of the deposition process yields even more complex optical microstructures: when omitting the lift-off step, the photoresist layer is combusted during the dewetting process of the thin gold film, leaving gold nanoparticles on both areas with and without photoresist but with a small, particle-free gap at the edge between the two areas (Figure 4f,g), providing a clear contrast at the edges of the pattern only (Figure 4h,i).

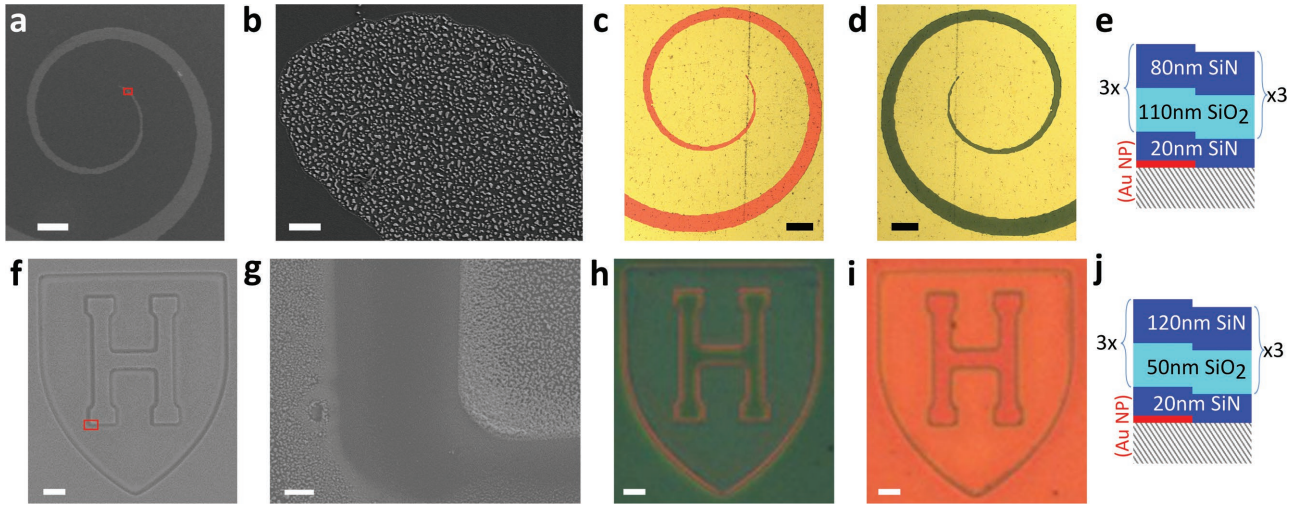

Figure 4. Spatially patterned optical Janus properties by local control of absorber deposition. a) SEM image of a single pattern showing the locations of the nanoparticles (bright areas). b) Higher resolution SEM image of the boxed region in (a) showing the nanoparticle size distribution. c) Optical microscopy image of the coating side of a patterned layer of gold nanoislands created using the method described in the text. d) Optical microscopy image of the same sample viewed from the substrate side. e) Schematic showing the thicknesses of the seven-layer film deposited on the patterned nanoparticle structure used for the generation of patterns shown in a-d. f–j) Same as (a–d) but for a sample made without the lift-off step, such that the gold nanoislands are located everywhere except for the edge of the micropattern, providing the contrast only at the small regions outlining the pattern. Scale bars: a,c,d) 400 µm; b) 1 µm; f,h,i) 10 µm; g) 1 µm.

The optical Janus effect can be created using absorbing elements with a large range of complex RIs, as indicated in Figure 2c,d. By overlaying the complex refractive index of commonly used metal films into the diagrams, we predict that plain metal or metalloid films used as absorbing element, e.g., chromium or germanium, can produce strongly asymmetric coloration, enabling simple, scalable, and cost-efficient fabrication processes. This procedure is very different from and has advantages over the previous method, which relied on nanoparticles for the absorbing element. Since the nanoparticles' optical properties can vary from batch to batch for synthesized particles and especially for in situ dewetted nanoparticles, the transfer matrix method simulation to calculate the exact color of the structure has to be tuned for every batch; thus, the colors of the material cannot be precisely designed a priori. If thin metal films are used instead, the RIs of the absorbing material can simply be looked up in a reference material, and the ability to rationally design the structures before fabrication is greatly increased.

As an example, in **Figure 5**a–c we show a patterned optical Janus stack comprised of two bilayers of SiO_2/SiN on top of a patterned chromium film on a glass slide. Similar to the gold nanoparticles used above, the large complex refractive index of a chromium thin film induces anomalous phase shifts upon reflection, giving rise to the observed structural color asymmetry. The choice of chromium as an absorbing material was motivated by its high complex RI (see Figure 2c–f), ease of deposition, high adhesion to the substrate, low cost, and lower number of processing steps required to produce patterned samples as compared to the dewetted gold nanoparticle layers mentioned previously. In the example, the structure was designed such that when viewed from the coating side, the pattern would be similar in color to the surrounding Bragg stack color without the absorbing layer, but when viewed from the substrate side, would display strong contrast with the background. This creates a viewing-direction-selective invisibility of the pattern (Figure 5a–c). An even more complex optical Janus effect is achieved by varying the thickness of the first layer deposited on top of the absorbing layer. Designing the Bragg stack in such a way that its peak wavelength is near the middle of the visible spectrum, we create a sample with short color travel when viewed from the front side, while displaying a range of colors when viewed from the substrate side (Figure 5d–f).

It should be noted that in all of the analytical calculations and experimental measurements in this paper, we have reported only normal incidence reflection spectra for the samples. The transmission spectra of Janus stacks must, by reciprocity, be identical regardless of the illumination direction.[26] The angle-dependence of these structures is similar to that of pure-dielectric multilayers in that there is a blueshift at increasing angles, as can be seen in Figure S8 and S9 (Supporting Information).

To conclude, we have designed and demonstrated semi-transparent materials having a different color depending on the viewing direction, by rationally combining absorbing and structural photonic elements. The physical origin of this optical Janus effect lies in the anomalous phase shift of reflected light caused by the complex RI of the absorbing material. In the stack, the dielectric environment of the absorbing material is anisotropic, leading to a different color from constructive interference on both sides of the sample, which can be predicted by transfer matrix calculations. The optical Janus effect is observed in a wide range of constituent photonic and absorbing elements. These include thin films and multilayer structures as the photonic elements and gold nanoparticles and plain metal films as the absorbing elements. Spatial control of the location of the absorbing elements enables the creation of arbitrary asymmetric structural color patterns with controllable, viewing-direction-dependent coloration as well as more complex anisotropic

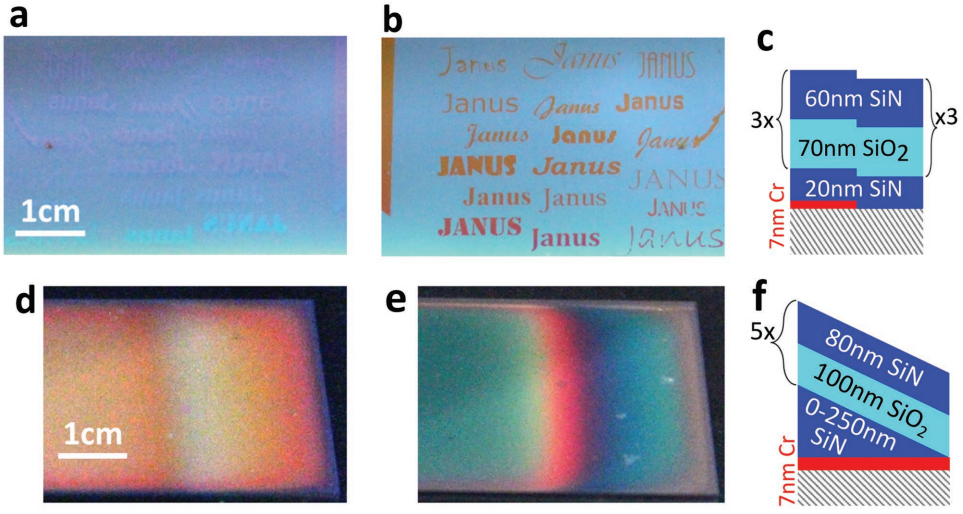

Figure 5. Viewing-direction-dependent optical effects from Janus coatings using a thin metal film as the absorbing element. a–c) Partially invisible Janus color patterns. a) Photograph of the coating side surface of a micropatterned asymmetric structural color stack designed to match colors of the features and the background from the coating side and thus hide the pattern. b) Photograph of the substrate side surface of the sample in (a) showing a high contrast between the color in the regions containing chromium and the color of the simple Bragg stack. c) Schematic showing the materials and thicknesses of the sample in (a,b). d–f) Viewing-direction-dependent polychromaticity from gradient thickness optical Janus films. d) Photograph of the structure showing a near solid orange color when viewed from the coating side. e) Same sample, but photographed from the substrate side, revealing a rainbow pattern in the region of the thickness gradient. f) Schematic showing the materials and thicknesses of the sample in (d,e).

effects such as viewing-direction-dependent invisibility of patterns or color travel. This rational design of asymmetric colored materials enables applications in art, architecture and design, and it may also allow more functional properties, for example in integrated photonic circuits, semitransparent solar cells with independent tunability of absorption profile and transmission color, or security features in anticounterfeiting materials.

Supporting Information

Supporting Information is available from the Wiley Online Library or from the author.

Acknowledgements

The work was supported by the National Science Foundation (NSF) under the Award No. DMREF-1533985. Fabrication was carried out at the Harvard Center for Nanoscale Systems, which is supported by the NSF's Materials Research Science and Engineering Centers Program DMR-1420570. N.V. acknowledges the support of the Cluster of Excellence Engineering of Advanced Materials (EAM) and of the Interdisciplinary Center for Functional Particle Systems (FPS) at Friedrich-Alexander University Erlangen-Nürnberg. The authors would like to thank Orad Reshef, Alexander Tesler, Alison Grinthal, Anna Shneidman, and Peter Korevaar for helpful discussions. G.T.E., N.V., and J.A. designed research. C.R. and E.S. synthesized nanoparticles. G.T.E., C.R., T.K., and E.S. fabricated samples. G.T.E. and C.R. measured samples. G.T.E. performed calculations. G.E., N.V., and J.A. wrote the manuscript. All the authors discussed and reviewed the manuscript.

Conflict of Interest

The authors declare no conflict of interest.

Keywords

absorption, multilayers, photonic crystals, structural color, thin films

Received: December 20, 2016
Revised: February 26, 2017
Published online:

[1] M. R. Gartia, A. Hsiao, A. Pokhriyal, S. Seo, G. Kulsharova, B. T. Cunningham, T. C. Bond, G. L. Liu, *Adv. Opt. Mater.* **2013**, *1*, 68.
[2] K. A. Duncan, C. Johnson, K. McElhinny, S. Ng, K. D. Cadwell, G. M. Zenner Petersen, A. Johnson, D. Horoszewski, K. Gentry, G. Lisensky, W. C. Crone, *J. Chem. Educ.* **2010**, *87*, 1031.
[3] F. J. Maile, G. Pfaff, P. Reynders, *Prog. Org. Coat.* **2005**, *54*, 150.
[4] M. Ferrara, M. Bengisu, *Materials That Change Color: Smart Materials, Intelligent Design*, Springer International Publishing **2014**.
[5] L. Zhu, J. Kapraun, J. Ferrara, C. J. Chang-Hasnain, *Optica* **2015**, *2*, 255.
[6] C. G. Granqvist, *Thin Solid Films* **2014**, *564*, 1.
[7] G. England, M. Kolle, P. Kim, M. Khan, P. Munoz, E. Mazur, J. Aizenberg, *Proc. Natl. Acad. Sci. USA* **2014**, *111*, 15630.
[8] L. Duempelmann, A. Luu-Dinh, B. Gallinet, L. Novotny, *ACS Photonics* **2016**, *3*, 190.
[9] a) M. A. Kats, R. Blanchard, P. Genevet, F. Capasso, *Nat. Mater.* **2013**, *12*, 20; b) M. A. Kats, S. J. Byrnes, R. Blanchard, M. Kolle, P. Genevet, J. Aizenberg, F. Capasso, *Appl. Phys. Lett.* **2013**, *103*, 101104; c) N. N. Shi, C. C. Tsai, F. Camino, G. D. Bernard, N. Yu, R. Wehner, *Science* **2015**, *349*, 298; d) M. M. Hossain, B. Jia, M. Gu, *Adv. Opt. Mater.* **2015**, *3*, 1047.
[10] a) I. B. Burgess, N. Koay, K. P. Raymond, M. Kolle, M. Loncar, J. Aizenberg, *ACS Nano* **2012**, *6*, 1427; b) K. R. Phillips, G. T. England, S. Sunny, E. Shirman, T. Shirman, N. Vogel, J. Aizenberg, *Chem. Soc. Rev.* **2016**, *45*, 281.
[11] S. Eustis, M. A. El-Sayed, *Chem. Soc. Rev.* **2006**, *35*, 209.
[12] V. Myroshnychenko, J. Rodriguez-Fernandez, I. Pastoriza-Santos, A. M. Funston, C. Novo, P. Mulvaney, L. M. Liz-Marzan, F. J. Garcia de Abajo, *Chem. Soc. Rev.* **2008**, *37*, 1792.
[13] a) P. Vukusic, J. R. Sambles, *Nature* **2003**, *424*, 852; b) L. Wu, J. He, W. Shang, T. Deng, J. Gu, H. Su, Q. Liu, W. Zhang, D. Zhang, *Adv. Opt. Mater.* **2016**, *4*, 195; c) T. Starkey, P. Vukusic, *Nanophotonics* **2013**, *2*, 289.
[14] D. Lin, P. Fan, E. Hasman, M. L. Brongersma, *Science* **2014**, *345*, 298.
[15] a) G. von Freymann, V. Kitaev, B. V. Lotsch, G. A. Ozin, *Chem. Soc. Rev.* **2013**, *42*, 2528; b) J. F. Galisteo-López, L. K. Gil, M. Ibisate, C. López, in *Organic and Hybrid Photonic Crystals*, (Ed: D. Comoretto), Springer International Publishing, Cham, Switzerland **2015**, p. 31.
[16] a) P. Tzeng, D. J. Hewson, P. Vukusic, S. J. Eichhorn, J. C. Grunlan, *J. Mater. Chem. C* **2015**, *3*, 4260; b) H. Shen, Z. Wang, Y. Wu, B. Yang, *RSC Adv.* **2016**, *6*, 4505.
[17] a) N. Koay, I. B. Burgess, T. M. Kay, B. A. Nerger, M. Miles-Rossouw, T. Shirman, T. L. Vu, G. England, K. R. Phillips, S. Utech, N. Vogel, M. Kolle, J. Aizenberg, *Opt. Express* **2014**, *22*, 27750; b) D. P. Josephson, E. J. Popczun, A. Stein, *J. Phys. Chem. C* **2013**, *117*, 13585; c) N. Vogel, S. Utech, G. T. England, T. Shirman, K. R. Phillips, N. Koay, I. B. Burgess, M. Kolle, D. A. Weitz, J. Aizenberg, *Proc. Natl. Acad. Sci. USA* **2015**, *112*, 10845; d) O. L. Pursiainen, J. J. Baumberg, H. Winkler, B. Viel, P. Spahn, T. Ruhl, *Opt. Express* **2007**, *15*, 9553.
[18] M. A. Kats, D. Sharma, J. Lin, P. Genevet, R. Blanchard, Z. Yang, M. M. Qazilbash, D. N. Basov, S. Ramanathan, F. Capasso, *Appl. Phys. Lett.* **2012**, *101*, 221101.
[19] J. Luo, S. Li, B. Hou, Y. Lai, *Sci. Rep.* **2016**, *6*, 28681.
[20] C. S. Park, V. R. Shrestha, S. S. Lee, D. Y. Choi, *Sci. Rep.* **2016**, *6*, 25496.
[21] S. Butun, K. Aydin, *ACS Photonics* **2015**, *2*, 1652.
[22] a) L. Duempelmann, D. Casari, A. Luu-Dinh, B. Gallinet, L. Novotny, *ACS Nano* **2015**, *9*, 12383; b) R. Yu, P. Mazumder, N. F. Borrelli, A. Carrilero, D. S. Ghosh, R. A. Maniyara, D. Baker, F. J. García de Abajo, V. Pruneri, *ACS Photonics* **2016**, *3*, 1194; c) K. Saito, T. Tatsuma, *Adv. Opt. Mater.* **2015**, *3*, 883.
[23] A. Walther, A. H. Muller, *Chem. Rev.* **2013**, *113*, 5194.
[24] A. Yariv, P. Yeh, *Photonics*, Oxford University Press, Oxford, UK **2006**.
[25] T. Karakouz, A. B. Tesler, T. A. Bendikov, A. Vaskevich, I. Rubinstein, *Adv. Mater.* **2008**, *20*, 3893.
[26] R. J. Potton, *Rep. Prog. Phys.* **2004**, *67*, 717.